THE JOURNAL OF BIOLOGICAL CHEMISTRY VOL. 286, NO. 11, pp. 9489–9502, March 18, 2011

Secretory Carrier Membrane Protein 2 Regulates Exocytic Insertion of NKCC2 into the Cell Membrane*

Received for publication, July 22, 2010, and in revised form, December 23, 2010 Published, JBC Papers in Press, January 4, 2011, DOI 10.1074/jbc.M110.166546

Nancy Zaarour[‡§¶1], Nadia Defontaine[‡§¶], Sylvie Demaretz[‡§¶], Anie Azroyan[‡§¶], Lydie Cheval[‡§¶], and Kamel Laghmani[‡§¶2]

From [‡]INSERM, Centre de Recherche des Cordeliers, UMRS 872, CNRS, ERL7226, 75006 Paris, France, [§]Université Pierre et Marie Curie, 75006 Paris, France, and the [¶]Faculté de Médecine, Université Paris-Descartes, 75005 Paris, France

The renal-specific Na-K-2Cl co-transporter, NKCC2, plays a pivotal role in regulating body salt levels and blood pressure. NKCC2 mutations lead to type I Bartter syndrome, a life-threatening kidney disease. Regulation of NKCC2 trafficking behavior serves as a major mechanism in controlling NKCC2 activity across the plasma membrane. However, the identities of the protein partners involved in cell surface targeting of NKCC2 are largely unknown. To gain insight into these processes, we used a yeast two-hybrid system to screen a kidney cDNA library for proteins that interact with the NKCC2 C terminus. One binding partner we identified was SCAMP2 (secretory carrier membrane protein 2). Microscopic confocal imaging and co-immunoprecipitation assays confirmed NKCC2-SCAMP2 interaction in renal cells. SCAMP2 associated also with the structurally related co-transporter NCC, suggesting that the interaction with SCAMP2 is a common feature of sodium-dependent chloride co-transporters. Heterologous expression of SCAMP2 specifically decreased cell surface abundance as well as transport activity of NKCC2 across the plasma membrane. Co-immunolocalization experiments revealed that intracellularly retained NKCC2 co-localizes with SCAMP2 in recycling endosomes. The rate of NKCC2 endocytic retrieval, assessed by the sodium 2-mercaptoethane sulfonate cleavage assay, was not affected by SCAMP2. The surface-biotinylatable fraction of newly inserted NKCC2 in the plasma membrane was reduced by SCAMP2, demonstrating that SCAMP2-induced decrease in surface NKCC2 is due to decreased exocytotic trafficking. Finally, a single amino acid mutation, cysteine 201 to alanine, within the conserved cytoplasmic E peptide of SCAMP2, which is believed to regulate exocytosis, abolished SCAMP2-mediated down-regulation of the co-transporter. Taken together, these data are consistent with a model whereby SCAMP2 regulates NKCC2 transit through recycling endosomes and limits the cell surface targeting of the co-transporter by interfering with its exocytotic trafficking.

NKCC2 is an Na-K-2Cl co-transporter protein expressed exclusively in the mammalian kidney, where it provides the major route for sodium/chloride transport across the apical plasma membrane of the thick ascending limb (1). NKCC2 is therefore a pivotal protein in renal function, and exquisitely tight regulation of the apical co-transporter activity is paramount for maintaining extracellular fluid volume and acid-base homeostasis (2). It is the target of loop-diuretics extensively used in the treatment of edematous states and hypertension (3). Furthermore, recent work implicates NKCC2 in the dysfunction of blood pressure regulation, raising new hypotheses regarding the underlying mechanisms behind some types of essential hypertension (4–7). Most importantly, inactivating mutations of the *NKCC2* gene in humans causes Bartter syndrome type 1, a life-threatening kidney disease (8). However, despite this importance, little is known about NKCC2 regulation in renal cells, mainly because of the difficulty in expressing the co-transporter protein in mammalian cells (9). As a consequence, although several studies have addressed various aspects of NKCC2 regulation (2, 7, 9–12), our knowledge of the molecular mechanisms underlying membrane trafficking of NKCC2 proteins in mammalian cells, in particular its regulation by protein-protein interactions, remain poor. Identifying and functionally characterizing a key and/or global protein interaction(s) and pathway(s) involved in the regulation of NKCC2 trafficking is important to understand its different physiological functions and dysfunctions.

NKCC2 belongs to the cation-chloride co-transporter (CCC)[3] family, which comprises two principal branches of membrane proteins (1). One branch includes the Na^+-dependent chloride co-transporters composed of the Na^+-K^+-$2Cl^-$ co-transporters (NKCC1 and NKCC2) and the Na^+-Cl^- co-transporter (NCC). The second branch includes the Na^+-independent K^+-Cl^- co-transporters. Members within this family are very homologous to one another, possessing 12 transmembrane-spanning domains, an N terminus of variable length, and a long cytoplasmic C terminus (2). Given that the C-terminal domain of NKCC2 is the predominant cytoplasmic region, it is likely to be a major factor in the trafficking of the NKCC2 protein. In support of this notion, we recently demonstrated that a highly conserved motif at the COOH terminus dictates endoplasmic reticulum exit and cell surface expression of NKCC2 (11). Moreover, there have been several reports demonstrating that the trafficking to the apical membrane of several ion trans-

* This work was supported by grants from INSERM (Paris, France).

[1] Recipient of a thesis fellowship from the Fondation pour la Recherche Médicale and from la Société de Neprologie.

[2] To whom correspondence should be addressed: UMRS 872-Equipe 3-ERL7226, 15 Rue de l'Ecole de Medecine, 752270 Paris Cedex 06, France. Tel.: 33-1-44-41-37-10; Fax: 33-1-44-41-37-17; E-mail: Kamel.Laghmani@crc.jussieu.fr.

[3] The abbreviations used are: CCC, cation-chloride co-transporter; TAL, thick ascending limb; MTAL, medullary TAL; CTAL, cortical TAL; EGFP, enhanced GFP; OKP, opossum kidney; aa, amino acid(s); NCC, NaCl co-transporter; HEK, human embryonic kidney; NHS, *N*-hydroxysuccinimide; NHE, Na^+-H^+ exchanger; MesNA, sodium 2-mercaptoethane sulfonate; TGN, *trans*-Golgi network.

port systems depend upon protein-protein interactions involving their extreme C terminus (13). For instance, deleting the last three residues of the cystic fibrosis transmembrane regulator chloride channel C terminus prevents its interactions with CAL, CAP70, and NHERF proteins and results in aberrant basolateral accumulation of the mutant protein (14–16). The interaction of NHERF proteins with the NHE-3 C terminus regulates the trafficking of the exchanger protein to the apical surface of proximal tubule cells (17). PDZ interactions mediated through the C-terminal tail of the Na-P_i co-transporter control its correct targeting to the renal proximal tubular brush border (18). Similar to NHE-3, cystic fibrosis transmembrane regulator chloride channel, and Na-P_i, NKCC2 surface expression is also subject to regulation by intracellular protein trafficking (19–21). However, very little is known about the protein-binding partners that control membrane sorting of NKCC2. More specifically, the identities of the protein partners of NKCC2 that orchestrate its exocytic insertion, endocytic retrieval, and recycling to and from the plasma membrane are scarcely known. Accordingly, identifying proteins that interact with the C-terminal tail of NKCC2 should help to further determine the mechanisms of regulated NKCC2 trafficking. In this report, we describe a novel protein-protein interaction between the C-terminal tail of NKCC2 and SCAMP2. SCAMP2 belongs to a family of evolutionarily conserved tetraspanning integral membrane proteins (22). To date, five isoforms of SCAMP (SCAMP1 to -5) have been identified in mammals and have been shown to be predominantly associated with recycling rather than degradation pathways (23–26). Indeed, SCAMPs are found mainly in the *trans*-Golgi network (TGN) and recycling endosomes and have been shown to play a role in endocytosis (26) and exocytosis (27, 28). Here, we show that SCAMP2 regulates the cell surface targeting of NKCC2 by controlling its exocytosis, revealing therefore a novel regulatory mechanism governing the trafficking of the co-transporter to the apical membrane.

EXPERIMENTAL PROCEDURES

Materials—All chemicals were obtained from Sigma unless otherwise noted. Penicillin and streptomycin were from Invitrogen. Subclonings were carried out with the following vectors: 1) pGKT7 (Clontech), 2) pCMV-Myc (Clontech), 3) pEGFP-C2 (Clontech), 4) pcDNA3.1/V5-His-TOPO (Invitrogen), and 5) pTarget (Promega, Madison, WI).

Yeast Two-hybrid Assay—Yeast two-hybrid screening was performed as described previously (29). Briefly, the cDNA fragment encoding the proximal region of the NKCC2 C terminus (first 108 aa) was cloned in-frame with the GAL4 DNA-binding domain in pGBKT7-BD and transformed into the yeast strain AH109. AH109 expressing the bait was then mated with the Y187 yeast strain pretransformed with a human kidney cDNA library constructed in the pACT2-AD vector. Mated yeast cells were first grown on low stringency selection plates (−Leu, −Trp, −His) and then on high stringency selection plates (−Leu, −Trp, −His, −Ade). Colonies were tested for β-galactosidase activity, and DNA from positive clones encoding the putative interacting proteins was isolated from yeast cells using the RPM yeast plasmid isolation kit (BIO 101 Systems). Prey plasmids were rescued by transformation into DH5 α bacteria (Invitrogen) and isolated using a Qiagen kit. Insert sizes were checked by BglII digestion. cDNA plasmids were then sequenced and assessed using the BLAST program.

Animals—Experiments were carried out on male C57BL/6J mice (8–10 weeks old; Charles Rivers Breeding Laboratories). Mice had free access to food (semisynthetic diet; SAFE, Epinay, France) and were allowed to drink water *ad libitum*.

All animals were treated in compliance with French and European Union animal care guidelines. All animal protocols were conducted in accordance with the European and French Research Council Guide for the Care and Use of Laboratory Animals and were approved by the review board of the Centre de Recherche des Cordeliers.

Isolation of Medullary and Cortical Thick Ascending Limb—After pentobarbital anesthesia (140 mg/g body weight, intraperitoneally), the left kidney was quickly perfused through the abdominal aorta with 5 ml of Hanks' modified microdissection solution and then with the same solution supplemented with 0.25% (w/v) collagenase (Serva, Heidelberg, Germany). The kidney was sliced along the cortico-papillary axis in small pieces, which were incubated for 10 min at 30 °C in collagenase-containing (0.15%, w/v) microdissection solution. After rinsing, medullary and cortical thick ascending limbs were dissected at 4 °C under stereomicroscopic observation and were identified by morphological and topographical criteria as described previously (30).

mRNA Extraction and Real-time RT-PCR Analysis—Total RNAs were extracted from pools of nephron segments (2–3 cm in length) using a Qiagen RNA extraction kit and reverse transcribed using the First-Strand cDNA synthesis kit for RT-PCR (Roche Applied Science), according to the manufacturer's protocol using random hexamers. Real-time PCR was performed on a LightCycler (Roche Applied Science) with either the LightCycler FastStart DNA Master SYBR Green 1 kit (Roche Applied Science) or the DyNAmo capillary SYBR Green quantitative PCR kit (Finnzymes, Ozyme, Saint Quentin en Yvelines, France), according to the manufacturers' protocols, except that the reaction volume was reduced 2.5-fold. PCR was performed with cDNA quantity corresponding to 0.2 mm of the different segments of nephron. No DNA was detectable in samples that did not undergo reverse transcription and in blanks run without cDNA. In each experiment, a standardization curve was made using serial dilutions of a standard cDNA stock solution made from either whole kidney or specific nephron segment RNA. Results (arbitrary units/mm tubule length) were normalized using *rpl26* as a reporter gene. Specific primers were designed using LightCycler ProbeDesign (Roche Applied Science). The sequences of the used primers were 5′-ATGTCGGCCTTCGACACTA-3′ (forward) and 5′-GTGTCGCAGGAACTGTTG-3′ (reverse) for SCAMP2, 5′-GCTAATGGCACAACCGTC-3′ (forward) and 5′-TCTCGATCGTTTCTTCCTTGTAT-3′ (reverse) for Rpl26, 5′-CAGTATGTCCAGACTGCATTG-3′ (forward) and 5′-AGATGGCCTGAGAAGGG-3′ (reverse) for claudin-2, and 5′-GAGATTGGCGTGGTCATAGTCAGAA-3′ (forward) and 5′-TGCTGCTGATGTTGCCGTCTTT-3′ (reverse) for NKCC2. Samples were submitted to 45 cycles of three temperature steps: 95 °C for 10 s, 60 °C for

20 s, and 72 °C for 13 s. In the experiment, a standardization curve was made using serial dilutions (1:1 to 1:500) of a cDNA stock solution from total kidney. The PCR products were size-fractionated on 2% agarose gels stained with ethidium bromide.

Constructs—The cDNAs encoding mouse NKCC2 and NCC co-transporters were fused at the N-terminal end of Myc (Myc-NKCC2, Myc-NCC) or EGFP (EGFP-NKCC2) using pCMV-Myc and pEGFP-C2 vectors, respectively. The mouse pendrin coding sequence was subcloned into pTarget mammalian expression vector. The human ClC-5, extracellularly HA-tagged and subcloned into the pTLN expression vector, was a gift from Dr. Stephane Lourdel (CRC des Cordeliers, Paris, France). The mouse SCAMP2 coding sequence was subcloned into the mammalian expression pcDNA3.1/V5 vector. Alanine substitutions were introduced into the SCAMP2-V5 construct at cysteine 201 (C201A) and tryptophan 202 (W202A) using the QuikChange mutagenesis system (Stratagene). All mutations were confirmed by sequencing.

Cell Culture—Opossum kidney (OKP) cells were grown in DMEM complemented with 10% fetal bovine serum (Invitrogen), penicillin (100 units/ml), and streptomycin (100 units/ml) at 37 °C in a humidified atmosphere containing 5% CO_2. Human embryonic kidney (HEK) 293 cells were maintained in DMEM supplemented with 10% fetal bovine serum and 1% penicillin/streptomycin. For DNA transfection, cells were grown to 60–70% confluence on plastic culture dishes and then were transiently transfected for 5 h with plasmids using the Lipofectamine Plus kit according to the manufacturer's instructions (Invitrogen).

Measurement of Intracellular pH and Na-K-2Cl Co-transporter Activity—Measurement of cytoplasmic pH (pH_i) was accomplished in cells grown to confluence on coverslips using the intracellularly trapped pH-sensitive dye 2′,7′-bis(carboxyethyl)-5,6-carboxyfluorescein. pH_i was estimated from the ratio of fluorescence with excitation wavelengths of 495 and 450 nm and emission wavelength of 530 nm (Horiba Jobin Yvon). Calibration of the 2′,7′-bis(carboxyethyl)-5,6-carboxyfluorescein excitation ratio was accomplished using the nigericin technique. Na-K-2Cl co-transport activity was measured as bumetanide-sensitive NH_4 influx, as described previously (29). Cells were first bathed at 37 °C in a CO_2-free Hepes/Tris-buffered medium, containing 135 mM NaCl, 10 mM Hepes (pH 7.4), 5 mM KCl, 1 mM $MgCl_2$, 0.8 mM KH_2PO_4, 0.2 mM K_2HOP_4, 1 mM $CaCl_2$, and 10 mM $BaCl_2$, to measure base-line pH_i. 20 mM NH_4Cl was then added to the medium, inducing a very rapid initial cellular alkalinization followed by a pH_i recovery. The initial rate of intracellular pH recovery (dpH_i/dt) was measured over the first 20 s of records, as reported earlier (29). The dpH_i caused by the addition of NH_4Cl was used to calculate the cell buffer capacity, which was not different between the studied groups (data not shown). Therefore, the Na-K-2Cl co-transporter activity is expressed as dpH_i/dt.

Protein Preparation, Immunoblotting, and Immunoprecipitation—Forty-eight hours after transfection, cells were washed three times with cold PBS and lysed in 0.2 or 0.5 ml of lysis buffer (120 mM Tris/Hepes, pH 7.4, 150 mM NaCl, 5 mM EDTA, 3 mM KCl, 1% (v/v) Triton X-100) containing protease inhibitors (Complete 1697498, Roche Applied Science). Samples were harvested, sonicated, and centrifuged at 16,000 rpm for 15 min at 4 °C. Protein expression levels were assessed after normalizing and loading equal amounts of total protein in 7.5% SDS-PAGE separation and Western blotting with the antibodies of interest. The primary antibodies used in the present study were the following: anti-V5 and anti-Rab11 (Invitrogen), anti-Myc (Clontech), anti-HA (Roche Applied Science), anti-SCAMP2 (Santa Cruz Biotechnology, Inc. (Santa Cruz, CA)), and anti-pendrin, a gift from Dr. D. Eladari (CRC des Cordeliers, Paris, France). For immunoprecipitation, cells were solubilized with lysis buffer containing 0.4 M NaCl, 0.5 mM EGTA, 1.5 mM $MgCl_2$, 10 mM Hepes, pH 7.9, 5% (v/v) glycerol, 0.5% (v/v) Nonidet P-40) and protease inhibitors (Complete, Roche Applied Science). Immunoprecipitation was carried out with the antibodies of interest, followed by affinity purification using protein G-agarose beads (Dynal). After incubation with protein G-agarose beads for 1 h at room temperature, the immunocomplex was washed three times in PBS (Invitrogen). The protein samples were boiled in loading buffer, run on gradient 6–20% SDS-polyacrylamide gels, and probed with primary antibodies of interest and horseradish peroxidase-conjugated secondary antibody, according to standard procedures. Proteins were visualized by enhanced chemiluminescence detection (PerkinElmer Life Sciences) following the manufacturer's instructions.

Biotinylation—Cells were placed on ice and rinsed twice with a cold rinsing solution containing PBS, pH 8, 1 mM $MgCl_2$, and 0.1 mM $CaCl_2$ (PBS-Ca-Mg). Cells were then gently agitated at 4 °C for 1 h in borate buffer, pH 9, containing 1 mg/ml NHS-biotin. Biotinylation was stopped by washing three times with ice-cold PBS supplemented with 100 mM glycine. Cells were then washed three times in PBS supplemented with 1 mM $MgCl_2$ and 0.1 mM $CaCl_2$. Washed cells were lysed for 45 min at 4 °C in solubilizing buffer (150 mM NaCl, 5 mM EDTA, 3 mM KCl, 120 mM Tris/Hepes, pH 7.4, 1% (v/v) Triton X-100) containing protease inhibitors (Complete 1697498, Roche Applied Science). After taking an aliquot of the total cell extract from each sample to provide a measure of total NKCC2 expression, the rest of cell lysates were incubated with avidin beads (Sigma) overnight at 4 °C. After overnight incubation, samples were centrifuged at 16,000 rpm for 5 min, and the supernatant (the intracellular fraction) was removed. Avidin beads were then washed with solubilizing buffer and then centrifuged for 7 min at 16,000 rpm seven times. Pellets were incubated in solubilizing buffer and denaturating buffer for 10 min at 95 °C and stored at −20 °C. Each fraction was subjected to SDS-PAGE and Western blot analysis.

Immunocytochemistry—Forty-eight hours after transfection, confluent cells were washed twice with PBS-Ca-Mg, pH 8. Cells were then incubated at 4 °C for 1 h in PBS-Ca-Mg, containing 1 mg/ml NHS-biotin. Cells were rinsed three times in rinsing solution with 100 mM glycine and reincubated at 4 °C in the same solution for 10 min. Then they were washed three times with PBS-Ca-Mg. Cells were fixed with 2% paraformaldehyde in PBS for 20 min at room temperature, incubated with 50 mM NH_4Cl, permeabilized with 0.1% Triton X-100 for 1 min, and incubated with DAKO (antibody diluent with background-reducing components) for 30 min to block nonspecific antibody

binding. Fixed cells were incubated for 1 h at room temperature with the primary antibodies at appropriate dilution in DAKO. For the transferrin uptake assay, cells were first starved overnight to deplete endogenous transferrin and growth factors. After a 60-min incubation at 37 °C with biotinylated holotransferrin to load recycling endosomes, cells were washed in ice-cold PBS and fixed as above. Washed cells were then mounted with Vectashield. Mouse anti-Myc and anti-V5 were visualized with Texas Red-coupled secondary antibodies. Rabbit anti-Myc, anti-Rab11, anti-Rab6, and anti-SCAMP2 were visualized with FITC-coupled IgG antibodies.

NKCC2 Endocytic Internalization—Measurement of NKCC2 endocytosis in OKP cells was performed with MesNa protection assays as described previously (31) with minor modifications. To inhibit endocytosis, cells were first put on ice in a 4 °C cold room and then washed twice with PBS-Ca-Mg, pH 8. OKP cells were surface-labeled with cleavable sulfo-NHS-SS-biotin and quenched as described above. All plates, except for that for the 0 min time point, were then flooded with prewarmed (37 °C) culture medium and returned to 37 °C for 15 or 30 min to allow endocytosis to proceed. At the end of each time period, samples were returned to the cold room to inhibit further endocytosis and were washed twice with PBS-Ca-Mg (pH 8) at 4 °C. Cells were then treated with MesNa (100 mM) in MesNa buffer (50 mM Tris, pH 8.6, 100 mM NaCl, 1 mM EDTA, 0.2% bovine serum albumin), a membrane-impermeable reducing agent, three times (for 15 min each) with gentle rocking at 4 °C. Under these conditions, only the biotin bound to freshly endocytosed proteins is protected from MesNa cleavage. Following treatment with MesNa, all plates were washed twice with PBS-Ca-Mg (pH 8) and then incubated in iodoacetamide (5 mg/ml) in PBS-Ca-Mg (pH 8) for 10 min at 4 °C. Cells were then lysed, and the biotinylated fraction, which represents nascent endocytosed surface protein, was precipitated with streptavidin-coupled agarose, and the precipitate was subjected to SDS-PAGE and blotting as described above.

NKCC2 Exocytic Insertion—Confluent quiescent OKP cells were rinsed with PBS as above and then exposed to 2 mg/ml sulfo-NHS-acetate in PBS-Ca-Mg for 2 h to saturate NHS-reactive sites on the cell surface as described (32). After quenching for 20 min (see above for quench conditions), cells were warmed to 37 °C for 1 h to permit protein trafficking. Cells were then surface-labeled with 1.5 mg/ml sulfo-NHS-SS-biotin and lysed as described above. The biotinylated fraction, which represents newly inserted surface proteins, was affinity-precipitated with streptavidin-coupled agarose, and the precipitate was subjected to SDS-PAGE and blotting with anti-Myc antibody as above.

Statistical Analyses—Results are expressed as mean ± S.E. Differences between means were evaluated using paired or unpaired *t* test or analysis of variance as appropriate. $p < 0.05$ was considered statistically significant.

RESULTS

Identification of SCAMP2 as a Novel NKCC2-interacting Protein—To identify novel NKCC2-interacting proteins, we used a yeast two-hybrid system to screen a human kidney cDNA expression library, employing a series of bait fragments spanning the predicted cytoplasmic C terminus (residues 661–1095) of murine NKCC2, as described in a previous report (29). Among the positive clones, one clone encoding full-length SCAMP2 was isolated as a candidate binding protein of the proximal region (first 108 aa, residues 661–768) of the NKCC2 C terminus. The interaction between SCAMP2 and NKCC2 was confirmed by retransforming the cloned cDNA into yeast using constructs issued from the yeast two-hybrid screening (Fig. 1*A*). To check for the specificity of the interaction between SCAMP2 and NKCC2 proteins, AH109 yeast cells were co-transformed with SCAMP2 and NKCC2 C1-term (residues 661–768) or NKCC2 C2-term (residues 741–909) (Fig. 1*A*, *left*). In contrast to results obtained with the proximal region of NKCC2 C terminus, no growth was observed when AH109 yeast cells were transformed with SCAMP2 and NKCC2 C2-term (Fig. 1*A*, *right*), indicating that the interaction is specific for the first 108 aa of the NKCC2 C terminus.

SCAMP2 Interacts with NKCC2 in Renal Cells—The above data clearly indicate that SCAMP2 interacts specifically with the proximal region of NKCC2 C terminus in yeast. To determine whether full-length NKCC2 might associate with SCAMP2 in a cellular context, the Myc-NKCC2 construct was transiently expressed either singly or in combination with SCAMP2-V5 in OKP cells. Cell lysates were incubated with anti-V5 or anti-Myc antibodies, and the resultant immunoprecipitates were resolved by SDS-PAGE and Western blot. As shown in Fig. 1*B*, *lanes 3* and *9*, immunoprecipitation of SCAMP2 followed by Western blotting for NKCC2 revealed robust co-immunoprecipitation of the two proteins, as illustrated by the intensity of the bands corresponding to NKCC2 proteins. The interaction appears to be specific because Myc-NKCC2 protein was not detected in control experiments in which OKP cells were not co-transfected with SCAMP2-V5 (*lanes 5* and *8*). However, heterologous expression systems may induce aggregation and nonspecific binding of proteins. To discount this possibility, we next tested whether endogenous SCAMP2 protein and NKCC2 interact in renal cultured cells. To address this question, we used a rabbit SCAMP2 antibody raised against native SCAMP2 protein. The efficiency and the specificity of this antibody were first tested by immunoprecipitation and Western blot analysis of cells overexpressing the SCAMP2-V5 construct. Both SCAMP2 and V5 antibodies detected the same band, similar to that showed in Fig. 1*B*, *lane 6*, thereby demonstrating the effectiveness of the antibodies in recognizing the SCAMP2 protein. Importantly, a single protein band around 38 kDa, corresponding to the expected size band of SCAMP2 (22, 33), was also obtained by Western blot analysis following immunoprecipitation with anti-SCAMP2 antibody, thus demonstrating the endogenous expression of SCAMP2 protein in OKP cells (Fig. 1*C*, *lane 3*). More importantly, immunoprecipitation of endogenous SCAMP2 protein brought down NKCC2, thus demonstrating physical interaction between the two proteins (Fig. 1*C*, *lane 3*). It is noteworthy that Myc-NKCC2 protein was not detected in control experiments in which in which immunoprecipitations were carried out using mouse anti-V5 or non-related antibodies (Fig. 1*C*, *lanes 2* and *4*). Taken in concert, these findings clearly indicate that NKCC2 interaction with SCAMP2 is not an artifact of the yeast

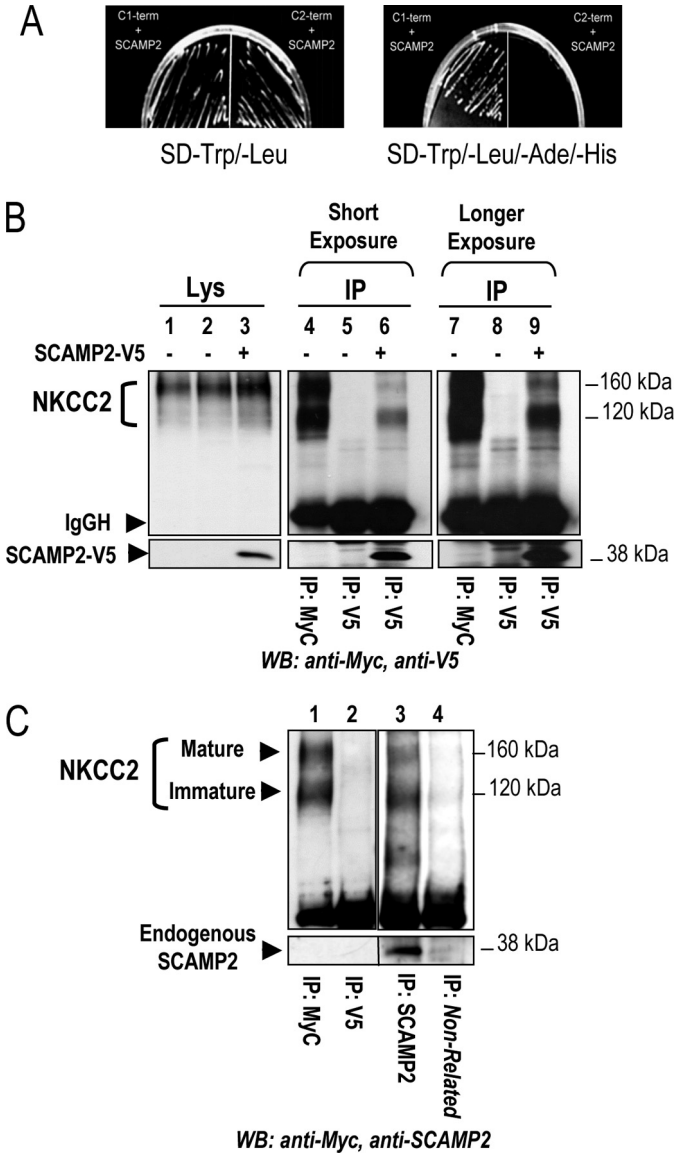

FIGURE 1. **Identification of SCAMP2 as a novel NKCC2-interacting protein.** *A*, SCAMP2 interacts with the proximal region of NKCC2 C terminus in yeast**.** Yeast two-hybrid analysis was performed using the Matchmaker system as described under "Experimental Procedures." The experiment demonstrates that co-expression of SCAMP2 and C1-term is required to support the growth of yeast in the absence of tryptophan, leucine, histidine, and adenine in the medium. This experiment also demonstrates the specific interaction between C1-term (but not C2-term) and SCAMP2. *B*, full-length NKCC2 interacts with SCAMP2 in OKP cells. OKP cells transiently expressing NKCC2 and SCAMP2 or NKCC2 alone were immunoprecipitated (*IP*) with anti-Myc (positive control; *lane 4*) antibody or anti-V5 anti-body (*lanes 5* and *6*). NKCC-2 co-immunoprecipitated with SCAMP2-V5 was detected by immunoblotting (*WB*) using anti-Myc (*lane 6*). 5% of total cell lysate (*Lys*) was resolved as positive control. *C*, endogenous SCAMP2 interacts with NKCC2. Cell lysates from OKP cells transiently transfected with Myc-NKCC2 were immunoprecipitated with anti-Myc or anti-V5 or non-related antibodies (negative control; *lanes 2* and *4*) or anti-SCAMP2 antibody (*lane 3*). Co-immunoprecipitated NKCC2 was detected by immunoblotting (*lane 3*). *IgGH*, the heavy chain of IgG.

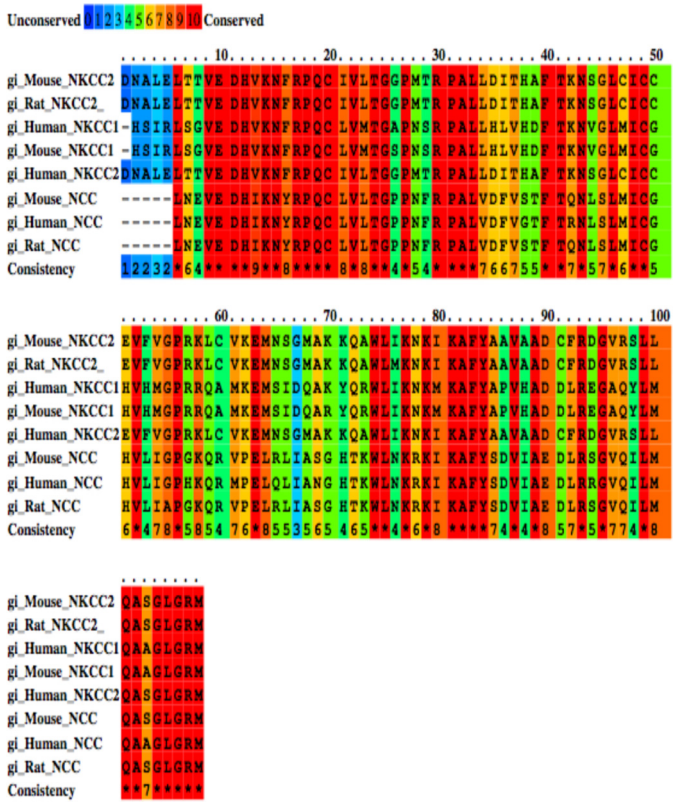

FIGURE 2. **Amino acid sequence alignment of the C termini (first 108 aa) of the NaCl co-transporter family, NKCC2, NKCC1, and NCC.** The conservation scoring was performed by PRALINE. The scoring scheme works from 0 for the least conserved alignment position, up to 10 for the most conserved alignment position.

two-hybrid system and that the two proteins really associate in *vivo*.

SCAMP2 Is a Common Binding Partner for NKCC2 and the Related NaCl Co-transporter, NCC—Sequence analysis of the first 108 aa of NKCC2 C terminus, the region interacting with SCAMP2 in yeast two-hybrid systems, revealed that it has considerable homology with other members of the sodium-dependent chloride co-transporter family, namely the ubiquitous Na-K-2Cl co-transporter isoform NKCC1 and the related kidney-specific electroneutral Na/Cl^- co-transporter NCC (Fig. 2). Indeed, this region is well conserved not only between all members of this family but also across species (Fig. 2), suggesting that SCAMP2 may be a common binding partner for NKCC1, NKCC2, and NCC. To verify this hypothesis, we tested the ability of SCAMP2 to interact with NCC in cultured renal cells. To this end, the co-transporter was N-terminally tagged with a Myc and transiently expressed in HEK and OKP cells in the presence or absence of SCAMP2-V5. Cell lysates were incubated with anti-V5 antibody, and the resultant immunoprecipitates were resolved by SDS-PAGE and Western blot. As with NKCC2, probing the blot with an anti-Myc antibody revealed NCC immunoreactive bands in immunoprecipitates from co-transfected cells (Fig. 3, *A* (*lane 4*) and *B* (*lane 6*)) but not from lysates of cells expressing only the co-transporter (Fig. 3, *A* (*lane 5*) and *B* (*lane 5*)), suggesting specific interaction between SCAMP2 and NCC. To further confirm the specificity of these interactions, we next checked, under the same experimental conditions, whether SCAMP2 could interact with ClC-5 and pendrin. ClC-5 (34) and pendrin (35) are two kidney chloride transporters that are not structurally related to NKCC2 and NCC. In contrast to the co-transporter proteins, neither ClC-5 (Fig. 3*C*, *lane 3*) nor pendrin (Fig. 3*D*, *lane 3*) could be recovered from SCAMP2 immunoprecipitates, thereby providing addi-

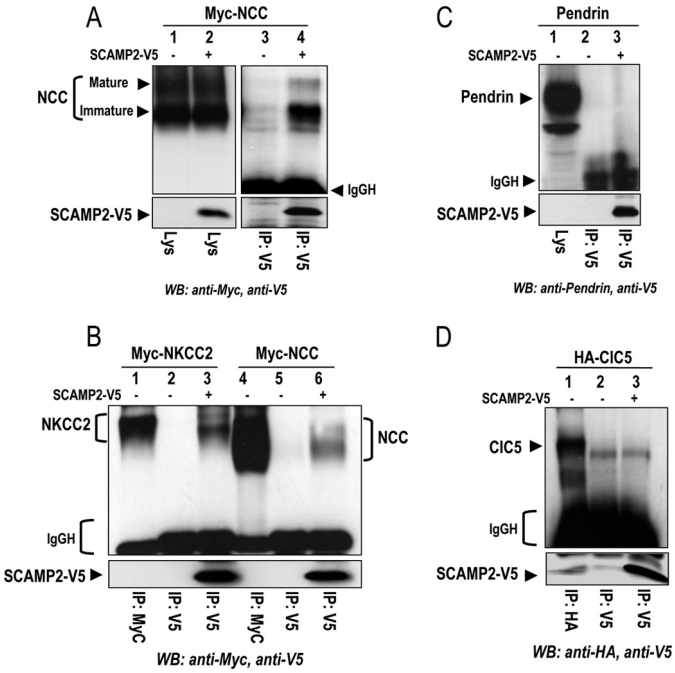

FIGURE 3. **SCAMP2 interacts specifically with NKCC2 and the related NaCl co-transporter NCC independently of the expression system.** Co-immunoprecipitation of SCAMP2 with NKCC2 and NCC in HEK cells (*A*) and OKP cells (*B*). Cell lysates from cells transiently transfected with Myc-NKCC2 or Myc-NCC in the presence or absence of SCAMP2-V5 were immunoprecipitated (*IP*) with anti-Myc or anti-V5 antibody. NCC co-immunoprecipitated with SCAMP2-V5 was detected by immunoblotting (*WB*) using anti-Myc (*lane 4*). 5% of total cell lysate (*Lys*) was resolved as positive control. *C* and *D*, SCAMP2 does not interact with pendrin and ClC-5. *C*, cell lysates from OKP cells transiently transfected with pendrin in the presence or absence of SCAMP2-V5 were immunoprecipitated with anti-V5 antibody. *Lane 1*, total cell lysate. In contrast to NKCC2 and NCC, pendrin protein was not recovered from SCAMP2 immunoprecipitates. *D*, cell lysates from HEK cells transiently transfected with HA-ClC-5 in the presence or absence of SCAMP2-V5 were immunoprecipitated with anti-HA (*lane 1*) or anti-V5 antibody (*lanes 2* and *3*). Similar to pendrin, ClC-5 protein was not detected in SCAMP2 immunoprecipitates. *IgGH*, the heavy chain of IgG.

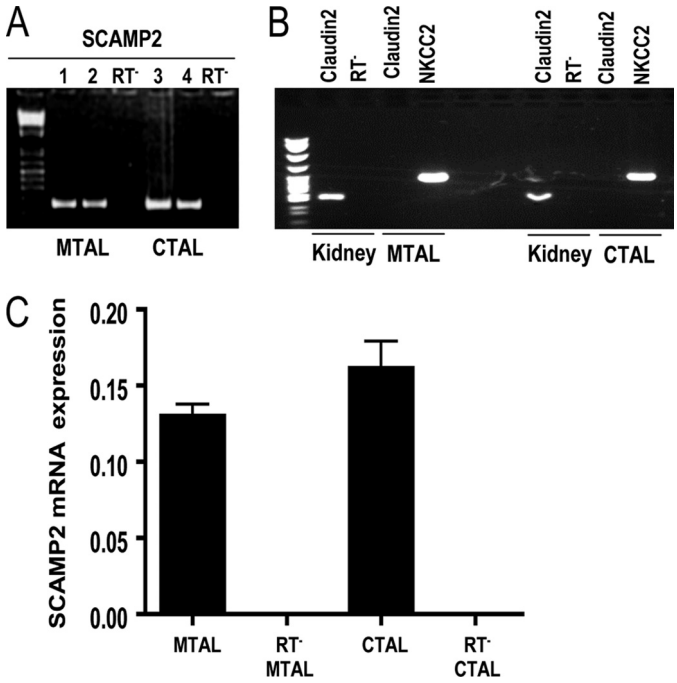

FIGURE 4. **SCAMP2 mRNA expression in TAL cells.** Real-time PCR and conventional RT-PCRs were carried out using specific primers of SCAMP2 sequence as described under "Experimental Procedures." *RT*(−), negative control of the RT-PCR without reverse transcriptase enzyme. *A*, reaction products obtained from real-time RT-PCR on MTAL (*lanes 1* and *2*) and CTAL (*lanes 3* and *4*) were separated using 2% agarose gel containing ethidium bromide. The expected size of the amplified SCAMP2 band was 152 bp. *B*, controls for the microdissection experiments; MTAL and CTAL samples were subjected to real-time RT-PCR to detect NKCC2 (TAL-positive marker) and claudin-2 (negative marker). For the claudin-2 reaction, a positive control was performed using total kidney homogenates. *C*, quantification of SCAMP2 reaction products obtained from real-time RT-PCR on MTAL and CTAL cells. Results (arbitrary units/mm tubule length) are expressed as means ± S.E. from several animals and normalized using *rpl26* as a reporter gene.

tional evidence for the specificity of the interaction of SCAMP2 with NCC and NKCC2 in renal cells.

Endogenous Expression of SCAMP2 in Native Thick Ascending Limb (TAL) Cells—The data described above show evidence that SCAMP2 interacts with NKCC2 in renal cultured cells. However, these findings will remain of disputable physiological importance if the two proteins are not expressed in the same cell types in native tissue. Indeed, as a precondition for establishing the physiological relevance of the observed interaction between NKCC2 and SCAMP2, it is necessary to show that both proteins are co-expressed in the same cells and exhibit overlapping distributions. To examine the expression of SCAMP2 in kidney TAL, we checked for the presence of its transcript in native TAL cells using real-time RT-PCR. Each reaction was performed on the equivalent of 0.2 mm of microdissected medullary (MTAL) and cortical (CTAL) TAL tubules. After amplification using a set of specific primers for SCAMP2, melting curve analysis revealed the expression of a single reaction product that, when separated using agarose gel electrophoresis (Fig. 4*A*), also yielded a single reaction product of the corresponding expected size (152 bp), thus indicating the expression of SCAMP2 in native MTAL and CTAL cells. No PCR product was obtained when reverse transcriptase was omitted from the reverse transcriptase reaction (Fig. 4, *A* and *C*). As can be seen in Fig. 4*C*, SCAMP2 mRNA expression was comparable between MTAL and CTAL cells. It is worth noting that under the same experimental conditions, control experiments using NKCC2 and claudin-2 (36) as positive and negative markers of TAL cells, respectively, were performed on the tested samples to ensure that SCAMP2 RT-PCR products, shown in Fig. 4*A*, originate from TAL cells (Fig. 4*B*). Taken together, these data clearly show that SCAMP2 is co-expressed with NKCC2 in both cortical and medullary TAL in the kidney.

NKCC2 and SCAMP2 Co-localize in Rab11-positive Compartments—To examine the subcellular distribution of NKCC2 and SCAMP2 complexes, we visualized with confocal microscopy the subcellular localization of EGFP-NKCC2 or Myc-NKCC2 protein, in the presence or absence of SCAMP2, in renal cultured cells. Of note, we have previously shown that, similar to Myc, N-terminal tagging of NKCC2 with EGFP does not affect the co-transporter trafficking (11, 29). As can be seen in Fig. 5*A*, in cells transfected with NKCC2 alone, the transporter partially co-localized with endogenous SCAMP2 in well defined structures in the prerinuclear region. In cells overexpressing both NKCC2 and SCAMP2, the two proteins co-localized also, mainly in the juxtanuclear region (Fig. 5, *B* and *B′*). It is worth mentioning that the perinuclear location of the NKCC2/SCAMP2-containing compartment is characteristic of

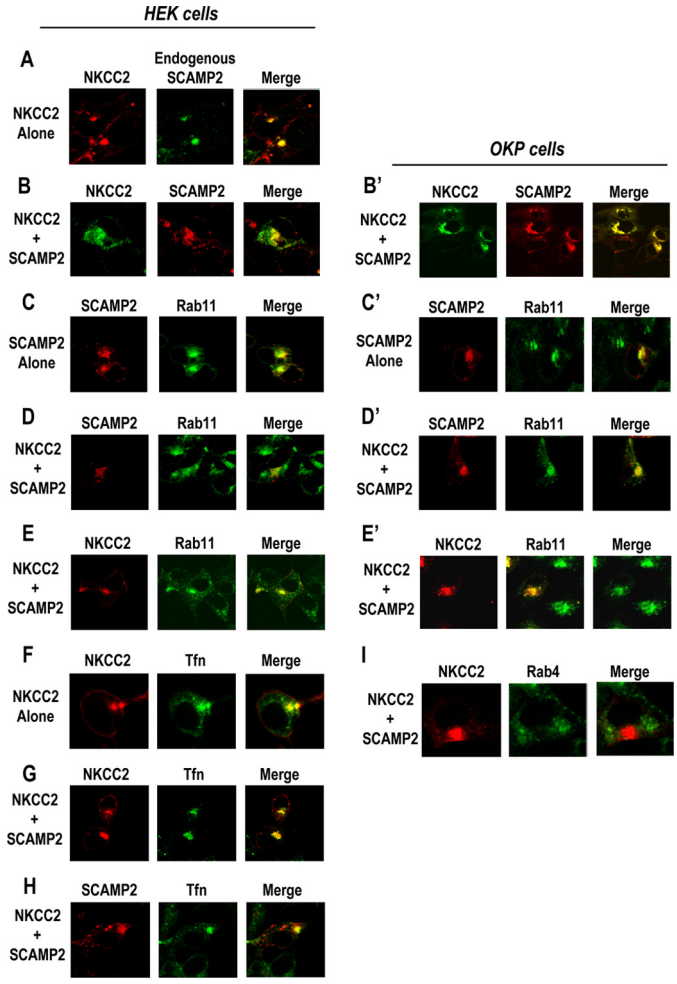

FIGURE 5. **SCAMP2 co-localizes with NKCC2 in Rab11-positive compartments.** *A*, endogenous SCAMP2 co-localizes with NKCC2. HEK cells transiently transfected with Myc-NKCC2 were double-stained with mouse anti-Myc (Texas Red) and rabbit anti-SCAMP2 (FITC) antibodies. *Yellow*, overlap between the Myc tag of NKCC2 protein (*red*) and SCAMP2 (*green*), representing co-localization of the proteins. *B* and *B'*, immunofluorescence confocal microscopy showing distribution of NKCC2 and SCAMP2 in HEK and OKP cells. OKP cells were transfected with NKCC2 N-terminally tagged with EGFP (*green*) or Myc with SCAMP2-V5. Fixed and permeabilized cells were stained with rabbit anti-Myc for NKCC2 (*green*) or mouse anti-V5 for SCAMP2 (Texas Red). The *yellow color* (*merged image*) indicates co-localization of the proteins. *C*, *C'*, *D*, *D'*, *E*, *E'*, *F*, *G*, and *H*, comparison between the distribution of NKCC2 and SCAMP2 and that of the recycling endosomal marker Rab11 and internalized transferrin. Transiently transfected cells with Myc-NKCC2 and/or SCAMP2-V5 proteins were stained with mouse anti-Myc for NKCC2 (Texas Red) or mouse anti-V5 for SCAMP2 (Texas Red) and rabbit anti-Rab11 (FITC, *green*). Internalized biotinylated holotransferrin was revealed with avidin-Cy2 (*green*). *I*, comparison between the distribution of NKCC2 and SCAMP2 and that of Rab4 (FITC, *green*). *Yellow* (*merged image*), co-localization of the proteins.

the endocytic recycling compartment in several cell types, including OK (37, 38) and HEK cells (39). These findings are of particular interest because a very recent study revealed that NKCC2 is recycled to the membrane in a constitutive manner, suggesting that the regulation of this trafficking pathway is very important for the regulation of surface NKCC2 levels (40). SCAMPs are also localized to the eukaryotic cell surface recycling system (23). Therefore, we next tested whether NKCC2 and SCAMP2 co-localize in recycling endosomes. Toward that end, we compared the distribution of NKCC2 and SCAMP2 with the recycling endosome marker Rab11 (41–46). As shown in Fig. 5, when expressed alone or in combination, SCAMP2 and NKCC2 co-localized with Rab11 in HEK and OKP cells (Fig. 5, *C*, *C'*, *D*, *D'*, *E*, and *E'*). Of note, the distribution of Rab11 was similar in adjacent (nontransfected) cells, indicating that overexpression of NKCC2-Myc and/or SCAMP2-V5 did not alter Rab11 targeting. In contrast to Rab11, the distribution of NKCC2 and SCAMP2 was clearly distinct from that of endogenous Rab4, another small GTPase that also controls the recycling process of certain membrane proteins from early endosomes to the plasma membrane (47) (Fig. 5*I*). Collectively, these data suggest that the recycling endosomes are the site of the SCAMP2-NKCC2 interaction. However, although widely used as a marker for recycling endosomes, Rab11 may also traffic between the *trans*-Golgi network and the cell surface (48). Thus, to better define the Rab11-positive perinuclear compartment in our studies, we also analyzed the extent to which NKCC2 co-localized with internalized transferrin, a marker for recycling endosomes that does not traffic to the Golgi. Transferrin is endocytosed upon binding to the transferrin receptor, is subsequently delivered to the recycling compartment, and then traffics back to the plasma membrane (43, 49). As shown in the merged images, NKCC2 and SCAMP2 co-localized with transferrin in a perinuclear location (Fig. 5, *F–H*). Of note, the subcellular localization of internalized transferrin was not seemingly different in cells expressing NKCC2 solely or in combination with SCAMP2, suggesting that SCAMP2 overexpression had no effect on transferrin trafficking. Most importantly, these findings provide additional evidence that NKCC2 and SCAMP2 interact, at least in recycling endosomes.

SCAMP2 Alters the Surface Expression of NKCC2—The interaction of SCAMP2 with NKCC2 in recycling endosomes raised the possibility that SCAMP2 might modulate NKCC2 targeting to the plasma membrane. To address this question, we first checked the effect of SCAMP2 co-expression on NKCC2 subcellular distribution in OKP cells. As shown in Fig. 6*A*, co-expressing SCAMP2 with NKCC2 apparently resulted in an alteration of subcellular distribution of the co-transporter protein. Indeed, in cells transfected with EGFP-NKCC2 alone, the co-transporter staining was primarily distributed in the plasma membrane, as indicated by co-localization with biotinylated cell surface proteins. Besides its cell surface expression, a fraction of the co-transporter was also located inside the cells, presumably representing transport intermediates en route to the cell surface (11). In cells co-expressing both proteins, a significant fraction of total NKCC2 appeared to be retained intracellularly. As a consequence, NKCC2 mostly disappeared from the cell membrane and clustered in an intracellular location (Fig. 6*A*). We therefore sought to study, in a more quantitative fashion, the effect of SCAMP2 on NKCC2 surface expression using cell surface biotinylation and streptavidin pull-down assays. To address this question, we transfected Myc-NKCC2 in the absence (empty vector) or presence of SCAMP2-V5 in OKP and HEK cells. Surface membrane proteins were biotinylated by reaction with sulfo-NHS-SS-biotin and isolated by precipitation with streptavidin-bound agarose. Myc-NKCC2 protein was then identified by immunoblot using anti-Myc antibody. We documented previously (29) that only the complex-glycosylated form of NKCC2 (160 kDa) is able to reach the

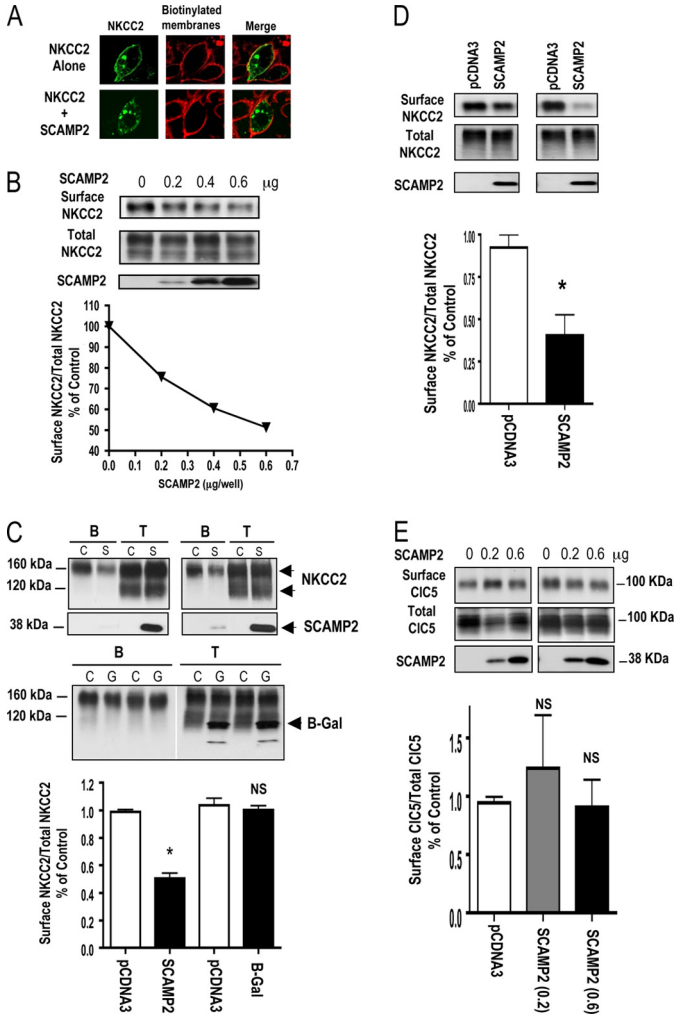

FIGURE 6. **SCAMP2 specifically decreases the amount of NKCC2 from the cell surface.** *A*, effect of SCAMP2 on subcellular distribution of NKCC2. OKP cells were transfected with pEGFP-NKCC2 (*green*) alone or with SCAMP2-V5. Membrane proteins of confluent cells were biotinylated at 4 °C with the biotinylation reagent sulfo-NHS-SS-biotin. Then the monolayers were fixed and stained for cell surface biotin (*avidin-Cy3*). The stained specimens were evaluated by confocal microscopy. Optical sections (*xy*) at the cell surface are depicted for the EGFP channel (*green*), Cy3 channel (*red*), and a merged channel. *B*, surface NKCC2 is reduced by SCAMP2 in a dose-dependent fashion. OKP cells were co-transfected with Myc-NKCC2 (0.2 μg/well) and increasing amounts of SCAMP2 OKP (0.2–0.6 μg/well) as indicated. Biotinylated proteins were recovered from cell extracts by precipitation with neutravidin-agarose. NKCC2 proteins on the cell surface were detected by Western blotting with Myc antibody. An aliquot of the total cell extract from each sample was also run on a parallel SDS gel and Western blotted for total NKCC2 expression. *Bottom*, densitometric analysis of total and surface NKCC2 is shown as the ratio of biotinylated to total NKCC2. Data are expressed as a percentage of control. *C*, cells were co-transfected with Myc-NKCC2 and the empty vector (*C*) or with SCAMP2-V5 (*S*) or β-galactosidase-V5 (*G*) cDNAs. *B*, biotinylated NKCC2. *T*, total NKCC2. *Bottom*, summary of results. *, $p < 0.0001$ *versus* NKCC2 alone (NKCC2 alone, $n = 8$; NKCC2 with SCAMP2, $n = 8$). *NS*, not significant *versus* NKCC2 alone (NKCC2 alone, $n = 3$; NKCC2 with β-gal, $n = 3$). *D*, surface NKCC2 is also reduced by SCAMP2 in HEK cells. HEK cells were co-transfected with Myc-NKCC2 (0.2 μg/well) alone or in combination with SCAMP2-V5 (0.6 μg/well). *Bottom*, summary of results. *, $p < 0.001$ *versus* NKCC2 alone. NKCC2 alone, $n = 4$. NKCC2 with SCAMP2, $n = 4$. *E*, SCAMP2-V5 overexpression has no effect on surface ClC-5. HEK cells were co-transfected with HA-ClC-5 (0.2 μg/well) alone or in combination with SCAMP2-V5 (0.2 or 0.6 μg/well). *Bottom*, summary of results. *NS*, not significant *versus* ClC-5 alone (ClC-5 alone, $n = 3$; ClC-5 with SCAMP2-V5, $n = 3$). *Error bars*, S.E.

apical surface. Consequently, in all experiments, the absence of high mannose type NKCC2 (120 kDa) was used as an indication of apical membrane integrity. When increasing amounts of SCAMP2 (0.2–0.6 μg/well) were co-expressed with NKCC2 (0.2 μg/well), NKCC2 surface expression was reduced in a dose-dependent manner (Fig. 6*B*). With 0.6 μg/well, SCAMP2 decreased NKCC2 surface expression by 49% ($p < 0.0001$) (Fig. 6*C*, *bottom*). Similar effects were observed in HEK cells (Fig. 6*D*). It is worth emphasizing that the SCAMP2-induced decrease in NKCC2 surface expression occurred in the absence of a decrease in the total cellular amount of NKCC2, rendering highly unlikely the possibility of nonspecific effects due to protein overexpression. This conclusion is further supported by the observation that, under identical conditions, co-transfecting β-galactosidase, a non-related protein, had no effect on the surface expression of NKCC2 (Fig. 6*C*).

Finally, we also examined the influence of SCAMP2 co-expression on the surface expression of ClC-5, which, unlike NKCC2, does not interact with SCAMP2 (Fig. 3*D*). In the kidney, ClC-5 is expressed in the plasma membrane and recycling endosomes (50–53). These control experiments were performed to examine the possibility that SCAMP2 may decrease the surface expression of NKCC2 by generally interfering with the migration of proteins through the trafficking pathway leading to the plasma membrane. As shown in Fig. 6*E*, co-expression of SCAMP2 with the ClC-5 had no effect on the surface expression of the latter. Accordingly, SCAMP2 is not simply disrupting the expression and targeting of integral plasma membrane proteins; rather, its inhibitory effect was specific for NKCC2. Collectively, these results demonstrate that SCAMP2 co-expression specifically decreases NKCC2 surface expression, an effect that probably stems from alterations in NKCC2 trafficking.

SCAMP2 Co-expression Reduces NKCC2 Transport Activity—To elucidate the functional consequence of SCAMP2-NKCC2 interactions and the observed reduction in the co-transporter surface expression, we then examined how co-expression of SCAMP2 affects NKCC2 activity in OKP cells. To this end, we transfected Myc-NKCC2 in the absence (empty vector) or presence of SCAMP2-V5 in OKP cells, and we examined NKCC2 transport activity. As previously described (11, 29, 54), to determine Na-K-2Cl co-transporter activity, we took advantage of the fact that NH_4^+ can be carried by this transporter by binding to its extracellular K^+-binding site. OKP cells were exposed to NH_4^+, and the rate of cell acidification following the initial cell alkalinization was studied as an index of NH_4^+ transport into the cells. The initial rate of intracellular pH recovery (dpH_i/dt), which is exclusively due to NH_4^+ entry, was measured over the first 20 s of records as reported earlier (11, 29). As can be seen in Fig. 7, Na-K-2Cl co-transporter activity decreased upon SCAMP2 co-expression (−52%, $p < 0.03$). Moreover, the presence of 0.1 mM bumetanide suppressed the initial rate of intracellular pH recovery in both groups, indicating that the NH_4^+-dependent pH_i recovery was due to the activity of the Na-K(NH_4^+)-Cl co-transporter. Taken together, these results clearly indicate that SCAMP2 co-expression decreases the activity of Myc-NKCC2 protein. Furthermore, the reduction in NKCC-2 transport activity (Fig. 7) clearly corresponds to the changes in NKCC2 levels at the cell surface (Fig. 6*C*), further strengthening the conclusion that SCAMP2 exerts its effect by causing a redistribution of NKCC-2 protein.

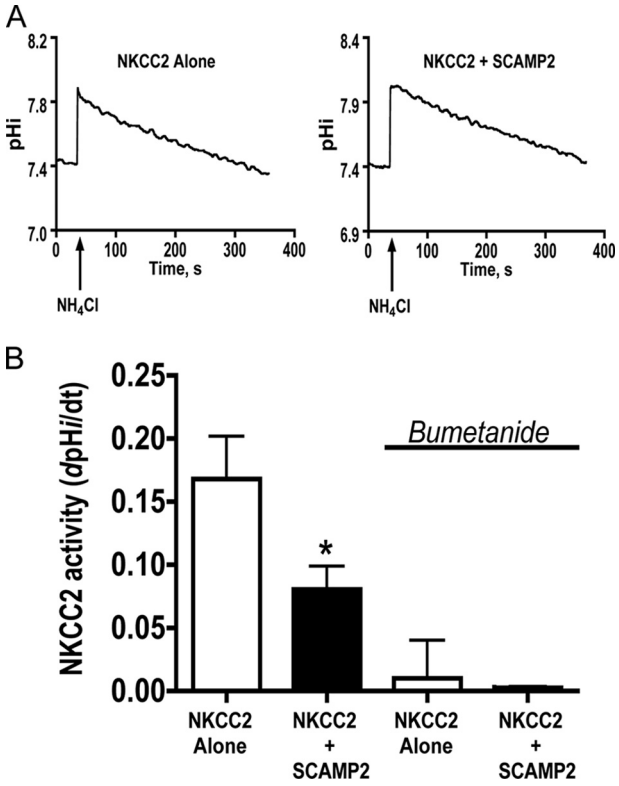

FIGURE 7. **SCAMP2 decreases NKCC2 transport activity.** Intracellular pH was measured in confluent monolayers of OKP cells as described under "Experimental Procedures." The *arrow* indicates replacement with medium containing 20 mM NH_4Cl (isosmotically substituted for NaCl). *A*, Na^+-$K^+(NH_4^+)$-$2Cl^-$ co-transport activity in OKP cells expressing Myc-NKCC2 (*blue*) in the absence (*left*) or presence (*right*) of SCAMP2. Results of representative experiments are shown. *B*, mean initial rate of pH_i recovery (dpH_i/dt) from an NH_4^+-induced alkaline load. Each *bar* represents the mean ± S.E. (*error bar*) rate of cell pH recovery (dpH_i/dt, pH units/min) under different experimental conditions (OKP cells expressing Myc-NKCC-2, OKP cells co-transfected with NKCC2 and SCAMP2, and OKP cells co-transfected with NKCC2 and SCAMP2 in the presence of 0.1 mM bumenatide). *, $p < 0.03$ *versus* NKCC2 alone (NKCC2 alone, $n = 3$; NKCC2 with SCAMP2, $n = 3$).

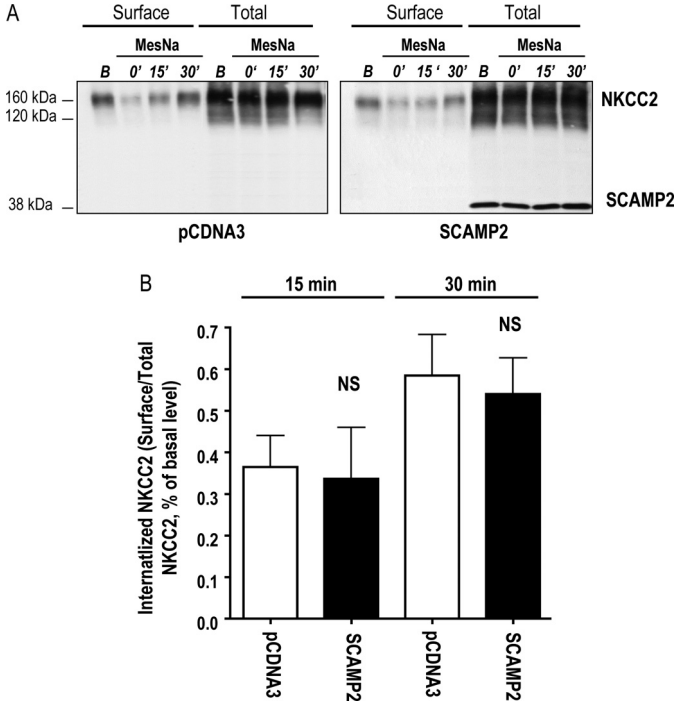

FIGURE 8. **SCAMP2 does not affect NKCC2 internalization.** *A*, typical blot. 48 h post-transfection of OKP cells with Myc-NKCC2 alone (with pcDNA empty vector) or with SCAMP2-V5, cell surface biotinylation was performed with sulfo-NHS-SS-biotin, followed by chase incubation in the culture media at 37 °C for 15 and/or 30 min to permit endocytosis of labeled proteins. Following the chase period, surface biotin was removed by incubation with MesNa, allowing visualization of internalized protein. Cells were then lysed; biotinylated proteins were purified by incubation with avidin-conjugated agarose beads and resolved by SDS-PAGE; and surface-labeled and -internalized Myc-NKCC2 was detected by Western blotting using an anti-Myc antibody (surface NKCC2). A small amount of total lysate (7%) was analyzed as a loading control and probed for SCAMP2-V5 and Myc-NKCC2 (total NKCC2, SCAMP2-V5). *B*, summary of all experiments ($n = 3$ for each group). The amount of Myc-NKCC2 internalized at each time point in pcDNA3- or SCAMP2-V5-transfected cells was compared directly with the untreated sample (basal surface NKCC2) from the same experiment, and therefore values are expressed as the mean after normalizing to basal levels. *NS*, not significant. *Error bars*, S.E.

SCAMP2-induced Decrease in Surface NKCC2 Is Due to Decreased Exocytotic Insertion—NKCC2 has been visualized in both the plasma membrane and intracellular compartments in native kidney tissue (55) as well as cultured cells (Fig. 6; see also Refs. 11 and 29). Therefore, the decrease in surface NKCC2 upon SCAMP2 co-expression can be caused by decreased exocytotic insertion, increased endocytotic retrieval, or synergetic combinations of these two processes. To measure endocytic internalization, we quantified the endocytotic rate biochemically with the MesNa protection assay. For this, 48 h after transfection of OKP cells with NKCC2 in the presence or absence of SCAMP2, surface proteins were first biotinylated with the reducible agent sulfo-NHS-SS-biotin. Cells were subsequently incubated at 37 °C for 15 or 30 min to allow endocytosis prior to MesNa treatment (Fig. 8*A*). With this protocol, biotinylated NKCC2 represents NKCC2 initially present on the plasma membrane and then endocytosed to be protected from MesNa. To assess the efficiency of MesNa cleavage, control experiments were performed immediately after biotinylation (time 0), and samples were kept at 4 °C and treated with MesNa. The remaining signal, which reflects incomplete cleavage of the NHS-biotin, was considered background and subtracted from the other bands treated with MesNa. As can be seen in Fig. 8, the rate of endocytosis of NKCC2 was not affected by SCAMP2, suggesting that reduction in NKCC2 surface expression by SCAMP2 is not due to increased endocytotic internalization.

We next studied the effect of SCAMP2 on the exocytotic insertion of NKCC2 in OKP cells. For this, 48 h after transfection of OKP cells with NKCC2 alone or in combination with SCAMP2, surface proteins accessible to NHS-SS-biotin were first masked by reaction with membrane-impermeant sulfo-NHS-acetate. Cells were then incubated at 37 °C for 1 h to permit protein trafficking, followed by biotinylation of cell surface proteins. Under these conditions, biotinylated NKCC2 represents NKCC2 that was located intracellularly at the beginning of the experiments (protected from sulfo-NHS-actetate) and on the cell surface at the end of the experiment. Controls were performed with omission of the 37 °C step, and any signal obtained denotes incomplete saturation of surface reactive sites with sulfo-NHS-acetate. Of note, when cells were kept at 4 °C to stop trafficking, a small amount of surface NKCC2 was visible. This probably reflects incomplete saturation of surface reactive sites with sulfo-NHS-acetate rather than exocytosis at 4 °C.

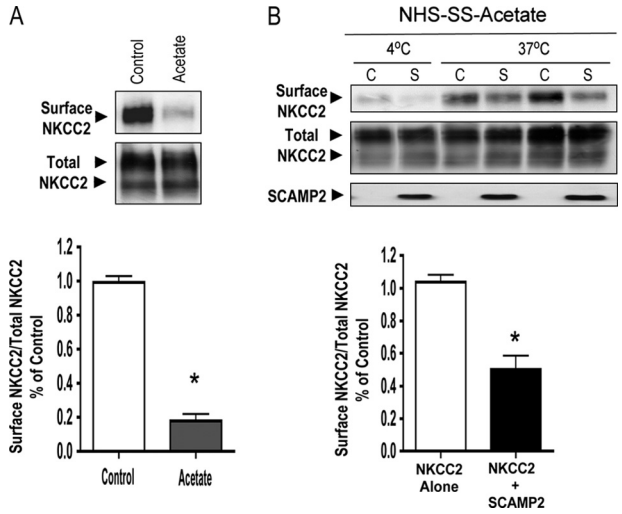

FIGURE 9. **SCAMP2 decreases NKCC2 exocytosis.** 48 h post-transfection, OKP cells expressing Myc-NKCC2 alone or with SCAMP2-V5 were labeled with sulfo-NHS-acetate. *A*, a representative Western blot shows surface (biotinylated) NKCC2 expression in OKP cells before (*first lane*; basal surface NKCC2) and after (*second lane*; 0 min at 37 °C) treatment with NHS-acetate to mask surface biotinylation sites. *B*, after masking, cells were maintained at 4 °C or incubated for 60 min at 37 °C. Cells were then cooled, and surface biotinylation was performed with sulfo-NHS-SS-biotin; biotinylated proteins were subsequently isolated by precipitation with streptavidin-bound agarose, and NKCC2 and SCAMP2 protein abundance was measured by immunoblot analysis with anti-Myc and anti-V5 antibodies, respectively. *Bottom*, summary of results. #, $p < 0.002$ *versus* control ($n = 3$). *, $p < 0.05$ *versus* NKCC2 alone ($n = 3$). *Error bars*, S.E.

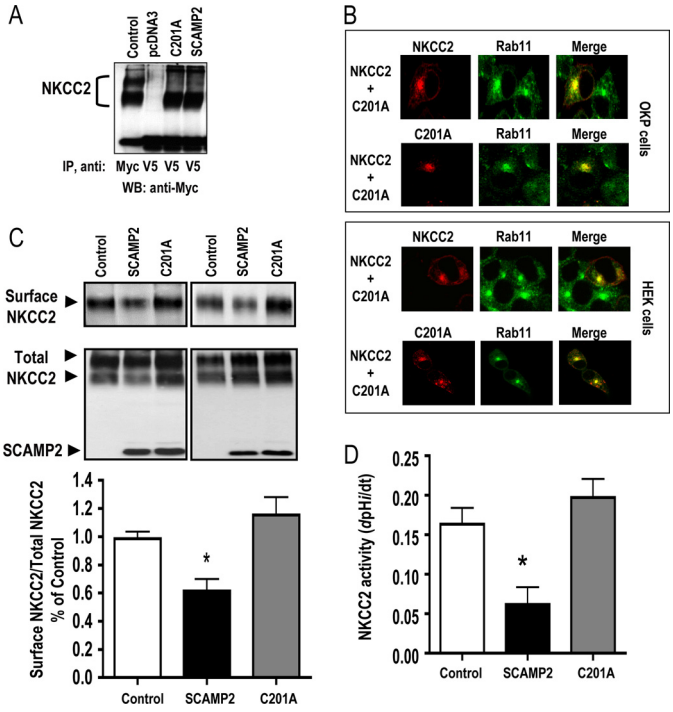

FIGURE 10. **Cysteine 201 within the E peptide of SCAMP2 is critical for the down-regulation of NKCC2 surface expression.** Experiments were performed in OKP cells expressing NKCC2 alone or NKCC2 with SCAMP2 or C201A. *A*, co-immunoprecipitation (*IP*) experiments on transfected OKP cells demonstrating that the single amino acid replacement in SCAMP2 does not abolish the interaction with NKCC2. *B*, effect of C201A mutation on NKCC2 surface expression, assessed by surface biotinylation as described above. *Bottom*, summary of all experiments. *, $p < 0.05$, *versus* NKCC2 alone (NKCC2 alone, $n = 6$; NKCC2 with SCAMP2, $n = 6$; NKCC2 with C201A, $n = 6$). *C*, comparison between the distribution of NKCC2 and C201A mutant and that of the recycling endosomal marker *Rab11*. Transiently transfected cells with Myc-NKCC2 and C201A proteins were stained with mouse anti-Myc for NKCC2 (Texas Red) or mouse anti-V5 for C201A (Texas Red) and rabbit anti-Rab11 (FITC, *green*). *Yellow* (*merged image*), co-localization of the proteins. *D*, mean initial rate of pH_i recovery (dpH_i/dt) from an NH_4^+-induced alkaline load. Each *bar* represents the mean ± S.E., rate of cell pH recovery (dpH_i/dt, pH units/min) under different experimental conditions (OKP cells expressing Myc-NKCC-2, OKP cells co-transfected with NKCC2 and SCAMP2, and OKP cells co-transfected with NKCC2 and C201A). *, $p < 0.05$, *versus* NKCC2 alone (NKCC2 alone, $n = 5$; NKCC2 with SCAMP2, $n = 4$; NKCC2 with C201A, $n = 6$). *Error bars*, S.E.

Overall, control experiments showed that NHS-acetate masked surface biotinylation by 82%, $p < 0.002$ (Fig. 9*A*). Under these conditions, we observed a decrease (−52%, $p < 0.05$) in newly labeled NKCC2 protein (Fig. 9*B*). Thus, SCAMP2 causes a decrease in the rate of exocytic insertion of NKCC2 into the cell membrane.

Cysteine 201 within the Highly Conserved E Peptide of SCAMP2 Is Required for the Down-regulation of NKCC2 Surface Expression—To identify the molecular determinants within SCAMP2 that are involved in the down-regulation of the co-transporter surface expression, we focused on the E peptide, which is believed to play a critical role in a late step in regulated exocytosis (27, 56). In particular, we initially focused on two residues within this E peptide, Cys^{201} and Trp^{202}, which play a pivotal role in this process (27, 56). To examine whether these residues are involved in the SCAMP2-mediated down-regulation of NKCC2, we generated two single amino acid mutations, C201A and W202A. However, the results of preliminary experiments revealed that the W202A mutant is expressed at lower levels when compared with wild type SCAMP2 protein, making it difficult to interpret the data obtained with this mutant. Therefore, in the subsequent experiments we focused mainly on the C201A mutant. We first tested the ability of mutated SCAMP2 proteins to interact with NKCC2 using co-immunoprecipitation assays on OKP cells transiently transfected with NKCC2 in combination with C201A. As shown in Fig. 10*A*, we were able to co-immunoprecipitate the NKCC2 protein in the presence of the C201A mutant, which implies that this residue does not participate in or influence the binding of SCAMP2 to NKCC2. In agreement with this observation, similar to WT SCAMP2, C201A mutant and NKCC2 co-localize in Rab11-positive compartments (Fig. 10*B*). We then compared the effects of the C201A protein on NKCC2 activity with those of WT SCAMP2. As illustrated in Fig. 10*C*, when Cys^{201} was individually mutated to alanine, SCAMP2 lost its ability to reduce the cell surface expression of NKCC2. Accordingly, in contrast to wild type SCAMP2, C201A mutant co-expression had no effect on NKCC2 transport activity (Fig. 10*D*). Of note, co-expression of the W202A mutant also had no effect on NKCC2 surface expression (data not shown). However, one cannot exclude the possibility that the inability of this mutant to down-regulate NKCC2 is due to the reduction of its protein expression. In contrast to W202A, we did not observe a difference in expression levels when comparing wild-type SCAMP2 and the C201A mutant protein, clearly indicating that the inability of the C201A mutant to reduce NKCC2 surface expression is mainly due to an impaired function of SCAMP2. Furthermore, the fact that a single amino acid replacement in SCAMP2 completely abolishes its effect on NKCC2 excludes, again, the possibility of nonspecific effects due to protein overexpression.

Collectively, these results provide supplemental proof that SCAMP2 co-expression specifically regulates the cell surface expression as well as the transport activity of NKCC2, an effect for which the Cys^{201} residue of SCAMP2 is indispensable.

DISCUSSION

In this study, we have identified SCAMP2 as a novel interacting partner of NKCC2 through yeast two-hybrid screening of a human kidney cDNA library. Our results indicate that SCAMP2 interaction with NKCC2 is specific and depends on the first 108 aa of the co-transporter C terminus. SCAMP2 binds also to the structurally related co-transporter NCC (2), suggesting that the interaction with SCAMP2 is a common feature of Na^+-dependent Cl^- co-transporters. Functional studies demonstrated that co-expression of SCAMP2 specifically decreases NKCC2 transport activity by promoting its intracellular retention and therefore reducing its abundance at the cell surface. SCAMP2-induced decrease in surface NKCC2 is due to decreased exocytic insertion.

SCAMP2 is a member of the evolutionarily conserved tetraspanning integral membrane proteins, which function as a carrier to the cell surface in post-Golgi recycling pathways (23, 57). In this report, we showed evidence for the specific binding of SCAMP2 to NKCC2. Using co-immunoprecipitation, we were able to detect the interaction *in vivo* between full-length NKCC2 and endogenous SCAMP2 protein in renal cells. Using yeast two-hybrid analysis, we observed that NKCC2 interaction with SCAMP2 is specific to the proximal region of the NKCC2 C terminus. This proximal region is highly conserved at the C termini of the Na^+-coupled Cl^--co-transporters NKCC1, NKCC2, and NCC. Accordingly, we were also able to show that SCAMP2 interacts with NCC. In contrast, ClC-5 and pendrin, two kidney chloride transporters (34, 35) that are not structurally related to the CCC family, failed to co-immunoprecipitate with SCAMP2, further supporting the specificity of the interaction of SCAMP2 with NCC and NKCC2 in renal cells. To identify the subcellular site of interaction of SCAMP2 with NKCC2, we visualized the subcellular distribution of the two proteins using confocal microscopy. NKCC2 and SCAMP2 showed considerable co-localization with endogenous Rab11, a commonly used marker of recycling endosomes (41–46). However, Rab11 has also been found to be associated with the TGN and post-Golgi vesicles (48, 58), indicating that the site of interaction between SCAMP2 and NKCC2 could be identified as recycling endosomes and/or TGN membranes. Because SCAMP2 and NKCC2 also co-localized with internalized transferrin, our data are consistent with the view that NKCC2 interacts with SCAMP2 in recycling endosomes. They are in agreement with a previous study showing that the internalized transferrin-containing vesicles are fused with a pre-existing internal pool of SCAMP-positive membranes and then accumulate in the SCAMP-rich perinuclear region corresponding to the recycling endosomal compartment (23). Also, a recent study by Diering and co-workers (59) reported considerable co-localization of SCAMP2 with Rab11 in recycling endosomes. Likewise, Müller and co-workers (60) demonstrated that SCAMP2-positive compartments contain the lipid raft marker follitin, supporting the idea that these structures could be also recycling endosomes. Thus, these findings together with our own suggest strongly that SCAMP2 interacts with NKCC2 in recycling endosomes. Of note, the co-immunoprecipitation experiments revealed that both immature and mature forms of NKCC2 interact with SCAMP2, which may serve as an indication that in addition to recycling endosomes, NKCC2 may also interact with SCAMP2 in other intracellular compartments, such as the endoplasmic reticulum. This possibility is further supported by previous observations reporting partial co-localization of NKCC2 (11) and SCAMP2 (33) with endoplasmic reticulum markers. However, some high mannose glycosylated proteins (immature) that are trafficked to the cell surface traverse the Golgi apparatus without further processing (61). As a consequence, for several membrane proteins, both immature and mature forms were detected at the plasma membranes (60, 62–64). Although only the mature form of NKCC2 is able to reach the cell surface, it is conceivable that, at least when using protein overexpression (62), a portion of immature wild type NKCC2 is delivered to post-Golgi compartments, including the TGN and recycling endosomes. Indeed, several reports provided evidence that recycling endosomes play a direct role in the biosynthetic pathway by serving as an intermediate during transport from the Golgi to cell plasma membranes (65–67). These observations therefore raise the possibility of an interaction between the immature form of NKCC2 and SCAMP2 in the recycling endosomes and/or the TGN. Nevertheless, regardless of the site of such an interaction, we did not observe any effect of SCAMP2 co-expression on immature NKCC2 protein. In contrast, we showed evidence that SCAMP2 is specifically involved in the regulation of the intracellular trafficking of the mature form of the co-transporter protein.

In support of trafficking as a regulator of NKCC2, previous immunolocalization experiments revealed that NKCC2 is expressed not only at the cell surface but also in a population of subapical vesicles (55). In the present study, using immunocytochemistry, we showed a similar subcellular localization of NKCC2 proteins in cultured renal cells. When expressed alone, NKCC2 was detected at the cell surface and in intracellular compartments. In contrast, in cells co-expressing SCAMP2, we observed enhanced intracellular accumulation of NKCC2 and a consequent reduction in the expression of the co-transporter at the cell surface. Indeed, upon SCAMP2 co-expression, a significant fraction of NKCC2 disappeared from the cell membrane and clustered in an intracellular location, where it exhibited excellent co-localization with SCAMP2. These data suggested that SCAMP2 binding alters NKCC2 trafficking to the cell surface. To corroborate this observation, we used surface biotinylation and showed that the co-transporter expression at the cell surface was reduced in a dose-dependent fashion by SCAMP2 in HEK and OKP cells. To investigate whether a general disruption of vesicular trafficking in our cultured renal cells may underlie the SCAMP2 effect, we studied the effect of SCAMP2 on ClC-5, because this kidney chloride transporter is also expressed at the plasma membrane and in recycling endosomes (50–53). In contrast to NKCC2, overexpressed SCAMP2 protein did not interact with ClC-5 and had no effect on ClC-5 surface expression. Hence, these data suggest that the SCAMP2-V5 construct does not generally disturb trafficking of

membrane proteins to and from the plasma membrane. Instead, it appears to specifically alter NKCC2 shuttling by interfering with its transit through recycling endosomes. Additional evidence for the specificity of SCAMP2 action on NKCC2 stems from the observation that SCAMP2 did not influence the distribution of Rab11 and internalized transferrin. Moreover, the specificity of SCAMP2-induced down-regulation of NKCC2 surface expression is also supported by a previous report demonstrating that NHE-5 interaction with overexpressed SCAMP2 in recycling endosomes promotes the cell surface targeting of the exchanger protein (59). Taken together, these findings suggest strongly that SCAMP2 specifically regulates NKCC2 transit through recycling endosomes to inhibit its cell surface targeting.

SCAMP2-induced down-regulation of NKCC2 membrane abundance could arise from a decrease in NKCC2 exocytosis to the plasma membrane and/or to an increase of NKCC2 endocytosis. To measure NKCC2 endocytic internalization, we prelabeled NKCC2 with sulfo-NHS-SS-biotin and then measured the ability of SCAMP2 to cause NKCC2 to shift to a location where the disulfide bond would be protected from MesNa. The results showed that 36 and 58% of surface NKCC2 is internalized over 15 and 30 min, respectively, and that SCAMP2 co-expression had no effect on the process. Hence, these studies suggest that the SCAMP2 effect on the amount of NKCC2 at the cell surface is not due to increased endocytotic internalization. To measure exocytic insertion of NKCC2, we preblocked surface proteins and then measured the ability to label new surface NKCC2 with biotin in the presence or absence of SCAMP2. The results showed that SCAMP2 induced a decrease in the exocytic insertion of NKCC2 into the plasma membrane. Studies by other investigators have shown that the function of SCAMP2 in regulated exocytosis involves the E peptide, a highly conserved segment lying at the cytosolic surface of the molecule and linking the second and the third transmembrane domains (22). In particular, two residues within the E peptide, Cys^{201} and Trp^{202}, were found to play a crucial role in this process (27, 56). In the present work, individual mutation of cysteine 201 to alanine reversed SCAMP2-mediated down-regulation of NKCC2. Remarkably, SCAMP2 mutant was able to co-immunoprecipitate with NKCC2 protein, implying that SCAMP2 interaction with NKCC2, *per se*, is not sufficient to alter the co-transporter surface expression. A similar mechanism has been reported in the regulation of SERT by SCAMP2 (60). Indeed, the authors of the latter study demonstrated that a point mutation in Cys^{201} abolishes SCAMP2-mediated reduction in the cell surface expression and activity of SERT without disturbing the interactions between the proteins. The precise molecular determinants of NKCC2 interaction with SCAMP2 remain to be resolved. Nevertheless, regardless of the mechanisms involved in such interactions, our data clearly indicate that SCAMP2 decreases exocytotic trafficking of NKCC2, thereby down-regulating the co-transporter abundance in the plasma membrane, an effect for which the SCAMP2 cysteine 201 residue is required.

Our findings implicate a role for SCAMP2 in the regulation of NKCC2 trafficking. However, very few if any proteins work in isolation. Appropriately, one may reasonably postulate that SCAMP2 works in concert with other NKCC2-binding proteins to create a synergetic effect on the co-transporter expression. In support of this idea, functional expression in *Xenopus laevis* oocytes showed that the C-terminal truncated isoform of NKCC2 reduced the co-transporter activity by preventing its arrival to the plasma membrane (68). Furthermore, we previously obtained evidence that aldolase binding to the proximal region of NKCC2 C terminus reduces NKCC2 surface expression (29). Additionally, the detection of NKCC2 proteins in Rab11-positive compartments, described here for the first time, may open new and important possibilities for studying the endocytic recycling and/or biosynthetic exocytotic membrane traffic of the co-transporter. Rab11, a small GTPase, is known to facilitate the recycling of membrane proteins from recycling endosomes to the plasma membrane (47). In addition to its role in recycling, several reports suggested a role for Rab11 in biosynthetic exocytotic membrane traffic by being directly involved in sorting from the TGN to the plasma membrane (58, 69). More specifically, Rab11 has been shown to remain associated with the exocytic vesicle during fusion with the plasma membrane, indicating that it is directly involved in exocytosis (45). Interestingly, a recent study demonstrated that Rab11 recycling of aquaporin 2 is an integral part of cAMP/vasopressin-induced trafficking of the channel to the plasma membrane (70). Based upon the above findings, it is conceivable that, in the basal state, NKCC2 accesses the cell surface from the recycling endosomes via a Rab11-dependent pathway. According to this view, SCAMP2 would regulate NKCC2 transit through the recycling endosomes and would inhibit exocytosis to the apical membrane by interfering with Rab11-dependent recycling and/or biosynthetic exocytotic membrane traffic. Moreover, similar to AQP2, *in vivo* and *in vitro* studies provided compelling evidence that cAMP/vasopressin induces the shuttling of NKCC2-containing vesicles to the cell membrane, thus leading to an increase in the surface expression of NKCC2 and its activity (19–21). This effect is mediated by enhanced exocytic insertion of the co-transporter into the apical membrane of TAL cells. Hence, it is tempting to speculate that the SCAMP2/Rab11-dependent pathway is also an integral part in the regulation of NKCC2 by cAMP/vasopressin. Consistent with this hypothesis, previous reports documented that NKCC2 (71) and SCAMP2 (60) proteins distribute in lipid rafts and that lipid rafts mediate cAMP/vasopressin-induced trafficking of the co-transporter (71). Obviously, these issues need to be examined directly.

In summary, we found that NKCC2 interacts specifically with SCAMP2, a post-Golgi-associated protein that is known to be involved in the regulation of vesicle transport. The interaction was confirmed by co-immunoprecipitation in renal cells. Co-immunofluorescence and biotinylation assays revealed that SCAMP2 interaction decreases NKCC2 exocytosis, therefore leading to retention and accumulation of the co-transporter in the cytoplasm. Identifying proteins that interact with kidney transporters and thereby regulate their expression is important to understand their differential physiological functions. To the best of our knowledge, this is the first study identifying a protein

partner of NKCC2 that plays a role in the co-transporter exocytotic trafficking. Consequently, these findings may open up new avenues in studying the regulation of the spatial distribution of kidney transporters in general and in particular of NKCC2 and NCC, proteins necessary for normal blood pressure homeostasis.

Acknowledgments—We thank Drs. Alain Doucet and Aurélie Edwards for helpful discussions and careful reading of the manuscript.

REFERENCES

1. Russell, J. M. (2000) *Physiol. Rev.* **80,** 211–276
2. Gamba, G. (2005) *Physiol. Rev.* **85,** 423–493
3. Gamba, G. (1999) *Kidney Int.* **56,** 1606–1622
4. Ashton, N. (2006) *J. Hypertens.* **24,** 2355–2356
5. Richardson, C., and Alessi, D. R. (2008) *J. Cell Sci.* **121,** 3293–3304
6. Gamba, G. (2005) *Am. J. Physiol. Renal. Physiol* **288,** F245–F252
7. Flatman, P. W. (2008) *Curr. Opin. Nephrol. Hypertens.* **17,** 186–192
8. Simon, D. B., and Lifton, R. P. (1996) *Am. J. Physiol.* **271,** F961–F966
9. Mount, D. B. (2006) *Am. J. Physiol. Renal. Physiol.* **290,** F606–F607
10. Carmosino, M., Giménez, I., Caplan, M., and Forbush, B. (2008) *Mol. Biol. Cell* **19,** 4341–4351
11. Zaarour, N., Demaretz, S., Defontaine, N., Mordasini, D., and Laghmani, K. (2009) *J. Biol. Chem.* **284,** 21752–21764
12. Hannemann, A., Christie, J. K., and Flatman, P. W. (2009) *J. Biol. Chem.* **284,** 35348–35358
13. Caplan, M. J. (1997) *Am. J. Physiol.* **272,** F425–F429
14. Cheng, J., Moyer, B. D., Milewski, M., Loffing, J., Ikeda, M., Mickle, J. E., Cutting, G. R., Li, M., Stanton, B. A., and Guggino, W. B. (2002) *J. Biol. Chem.* **277,** 3520–3529
15. Wang, S., Raab, R. W., Schatz, P. J., Guggino, W. B., and Li, M. (1998) *FEBS Lett.* **427,** 103–108
16. Wang, S., Yue, H., Derin, R. B., Guggino, W. B., and Li, M. (2000) *Cell* **103,** 169–179
17. Donowitz, M., Cha, B., Zachos, N. C., Brett, C. L., Sharma, A., Tse, C. M., and Li, X. (2005) *J. Physiol.* **567,** 3–11
18. Hernando, N., Déliot, N., Gisler, S. M., Lederer, E., Weinman, E. J., Biber, J., and Murer, H. (2002) *Proc. Natl. Acad. Sci. U.S.A.* **99,** 11957–11962
19. Giménez, I., and Forbush, B. (2003) *J. Biol. Chem.* **278,** 26946–26951
20. Ortiz, P. A. (2006) *Am. J. Physiol. Renal. Physiol* **290,** F608–F616
21. Caceres, P. S., Ares, G. R., and Ortiz, P. A. (2009) *J. Biol. Chem.* **284,** 24965–24971
22. Hubbard, C., Singleton, D., Rauch, M., Jayasinghe, S., Cafiso, D., and Castle, D. (2000) *Mol. Biol. Cell* **11,** 2933–2947
23. Castle, A., and Castle, D. (2005) *J. Cell Sci.* **118,** 3769–3780
24. Han, C., Chen, T., Yang, M., Li, N., Liu, H., and Cao, X. (2009) *J. Immunol.* **182,** 2986–2996
25. Liao, H., Zhang, J., Shestopal, S., Szabo, G., Castle, A., and Castle, D. (2008) *Am. J. Physiol. Cell Physiol.* **294,** C797–C809
26. Fernández-Chacón, R., Achiriloaie, M., Janz, R., Albanesi, J. P., and Südhof, T. C. (2000) *J. Biol. Chem.* **275,** 12752–12756
27. Guo, Z., Liu, L., Cafiso, D., and Castle, D. (2002) *J. Biol. Chem.* **277,** 35357–35363
28. Liao, H., Ellena, J., Liu, L., Szabo, G., Cafiso, D., and Castle, D. (2007) *Biochemistry* **46,** 10909–10920
29. Benziane, B., Demaretz, S., Defontaine, N., Zaarour, N., Cheval, L., Bourgeois, S., Klein, C., Froissart, M., Blanchard, A., Paillard, M., Gamba, G., Houillier, P., and Laghmani, K. (2007) *J. Biol. Chem.* **282,** 33817–33830
30. Doucet, A., Katz, A. I., and Morel, F. (1979) *Am. J. Physiol.* **237,** F105–F113
31. Hu, M. C., Fan, L., Crowder, L. A., Karim-Jimenez, Z., Murer, H., and Moe, O. W. (2001) *J. Biol. Chem.* **276,** 26906–26915
32. Yang, X., Amemiya, M., Peng, Y., Moe, O. W., Preisig, P. A., and Alpern, R. J. (2000) *Am. J. Physiol. Cell Physiol* **279,** C410–C419
33. Lin, P. J., Williams, W. P., Luu, Y., Molday, R. S., Orlowski, J., and Numata, M. (2005) *J. Cell Sci.* **118,** 1885–1897
34. Steinmeyer, K., Schwappach, B., Bens, M., Vandewalle, A., and Jentsch, T. J. (1995) *J. Biol. Chem.* **270,** 31172–31177
35. Mount, D. B., and Romero, M. F. (2004) *Pflugers Arch.* **447,** 710–721
36. Enck, A. H., Berger, U. V., and Yu, A. S. (2001) *Am. J. Physiol. Renal. Physiol.* **281,** F966–F974
37. Akhter, S., Kovbasnjuk, O., Li, X., Cavet, M., Noel, J., Arpin, M., Hubbard, A. L., and Donowitz, M. (2002) *Am. J. Physiol. Cell Physiol.* **283,** C927–C940
38. Hardel, N., Harmel, N., Zolles, G., Fakler, B., and Klöcker, N. (2008) *Cardiovasc. Res.* **79,** 52–60
39. Idkowiak-Baldys, J., Baldys, A., Raymond, J. R., and Hannun, Y. A. (2009) *J. Biol. Chem.* **284,** 22322–22331
40. Ares, G. R., and Ortiz, P. A. (2010) *Am. J. Physiol. Renal. Physiol.* **299,** F1193–F1202
41. Green, E. G., Ramm, E., Riley, N. M., Spiro, D. J., Goldenring, J. R., and Wessling-Resnick, M. (1997) *Biochem. Biophys. Res. Commun.* **239,** 612–616
42. Bartz, R., Benzing, C., and Ullrich, O. (2003) *Biochem. Biophys. Res. Commun.* **312,** 663–669
43. Ren, M., Xu, G., Zeng, J., De Lemos-Chiarandini, C., Adesnik, M., and Sabatini, D. D. (1998) *Proc. Natl. Acad. Sci. U.S.A.* **95,** 6187–6192
44. Wang, X., Kumar, R., Navarre, J., Casanova, J. E., and Goldenring, J. R. (2000) *J. Biol. Chem.* **275,** 29138–29146
45. Ward, E. S., Martinez, C., Vaccaro, C., Zhou, J., Tang, Q., and Ober, R. J. (2005) *Mol. Biol. Cell* **16,** 2028–2038
46. Hoekstra, D., Tyteca, D., and van IJzendoorn, S. C. (2004) *J. Cell Sci.* **117,** 2183–2192
47. Jones, M. C., Caswell, P. T., and Norman, J. C. (2006) *Curr. Opin. Cell Biol.* **18,** 549–557
48. Urbé, S., Huber, L. A., Zerial, M., Tooze, S. A., and Parton, R. G. (1993) *FEBS Lett.* **334,** 175–182
49. Sönnichsen, B., De Renzis, S., Nielsen, E., Rietdorf, J., and Zerial, M. (2000) *J. Cell Biol.* **149,** 901–914
50. Thakker, R. V. (2000) *Kidney Int.* **57,** 787–793
51. Mohammad-Panah, R., Harrison, R., Dhani, S., Ackerley, C., Huan, L. J., Wang, Y., and Bear, C. E. (2003) *J. Biol. Chem.* **278,** 29267–29277
52. Hryciw, D. H., Ekberg, J., Pollock, C. A., and Poronnik, P. (2006) *Int. J. Biochem. Cell Biol.* **38,** 1036–1042
53. Hryciw, D. H., Ekberg, J., Lee, A., Lensink, I. L., Kumar, S., Guggino, W. B., Cook, D. I., Pollock, C. A., and Poronnik, P. (2004) *J. Biol. Chem.* **279,** 54996–55007
54. Amlal, H., Legoff, C., Vernimmen, C., Paillard, M., and Bichara, M. (1996) *Am. J. Physiol.* **271,** C455–C463
55. Nielsen, S., Maunsbach, A. B., Ecelbarger, C. A., and Knepper, M. A. (1998) *Am. J. Physiol.* **275,** F885–F893
56. Liu, L., Guo, Z., Tieu, Q., Castle, A., and Castle, D. (2002) *Mol. Biol. Cell* **13,** 4266–4278
57. Fernández-Chacón, R., and Südhof, T. C. (2000) *J. Neurosci.* **20,** 7941–7950
58. Satoh, A. K., O'Tousa, J. E., Ozaki, K., and Ready, D. F. (2005) *Development* **132,** 1487–1497
59. Diering, G. H., Church, J., and Numata, M. (2009) *J. Biol. Chem.* **284,** 13892–13903
60. Müller, H. K., Wiborg, O., and Haase, J. (2006) *J. Biol. Chem.* **281,** 28901–28909
61. Vagin, O., Kraut, J. A., and Sachs, G. (2009) *Am. J. Physiol. Renal Physiol* **296,** F459–F469
62. Johns, T. G., Mellman, I., Cartwright, G. A., Ritter, G., Old, L. J., Burgess, A. W., and Scott, A. M. (2005) *FASEB J.* **19,** 780–782
63. Watanabe, I., Wang, H. G., Sutachan, J. J., Zhu, J., Recio-Pinto, E., and Thornhill, W. B. (2003) *J. Physiol.* **550,** 51–66
64. Zhu, J., Watanabe, I., Gomez, B., and Thornhill, W. B. (2003) *Biochem. J.* **375,** 761–768
65. Ang, A. L., Taguchi, T., Francis, S., Fölsch, H., Murrells, L. J., Pypaert, M., Warren, G., and Mellman, I. (2004) *J. Cell Biol.* **167,** 531–543
66. Cresawn, K. O., Potter, B. A., Oztan, A., Guerriero, C. J., Ihrke, G., Goldenring, J. R., Apodaca, G., and Weisz, O. A. (2007) *EMBO J.* **26,**

3737–3748
67. Ellis, M. A., Potter, B. A., Cresawn, K. O., and Weisz, O. A. (2006) *Am. J. Physiol. Renal. Physiol.* **291,** F707–F713
68. Meade, P., Hoover, R. S., Plata, C., Vázquez, N., Bobadilla, N. A., Gamba, G., and Hebert, S. C. (2003) *Am. J. Physiol. Renal. Physiol.* **284,** F1145–F1154
69. Lock, J. G., and Stow, J. L. (2005) *Mol. Biol. Cell* **16,** 1744–1755
70. Takata, K., Matsuzaki, T., Tajika, Y., Ablimit, A., and Hasegawa, T. (2008) *Histochem. Cell Biol.* **130,** 197–209
71. Welker, P., Böhlick, A., Mutig, K., Salanova, M., Kahl, T., Schlüter, H., Blottner, D., Ponce-Coria, J., Gamba, G., and Bachmann, S. (2008) *Am. J. Physiol. Renal. Physiol.* **295,** F789–F802